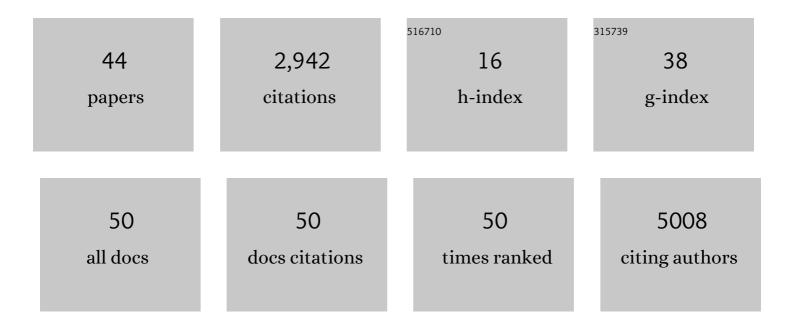
Oleh Dzyubachyk

List of Publications by Year in descending order

Source: https://exaly.com/author-pdf/7824633/publications.pdf Version: 2024-02-01



#	Article	lF	CITATIONS
1	Methods for Cell and Particle Tracking. Methods in Enzymology, 2012, 504, 183-200.	1.0	1,217
2	An objective comparison of cell-tracking algorithms. Nature Methods, 2017, 14, 1141-1152.	19.0	399
3	A benchmark for comparison of cell tracking algorithms. Bioinformatics, 2014, 30, 1609-1617.	4.1	345
4	Advanced Level-Set-Based Cell Tracking in Time-Lapse Fluorescence Microscopy. IEEE Transactions on Medical Imaging, 2010, 29, 852-867.	8.9	239
5	Tracking in cell and developmental biology. Seminars in Cell and Developmental Biology, 2009, 20, 894-902.	5.0	213
6	Iron loading is a prominent feature of activated microglia in Alzheimer's disease patients. Acta Neuropathologica Communications, 2021, 9, 27.	5.2	79
7	Automated analysis of time-lapse fluorescence microscopy images: from live cell images to intracellular foci. Bioinformatics, 2010, 26, 2424-2430.	4.1	38
8	Advanced level-set based multiple-cell segmentation and tracking in time-lapse fluorescence microscopy images. , 2008, , .		34
9	Clinically relevant timing of antenatal sildenafil treatment reduces pulmonary vascular remodeling in congenital diaphragmatic hernia. American Journal of Physiology - Lung Cellular and Molecular Physiology, 2016, 311, L734-L742.	2.9	32
10	Automated Ischemic Lesion Segmentation in MRI Mouse Brain Data after Transient Middle Cerebral Artery Occlusion. Frontiers in Neuroinformatics, 2017, 11, 3.	2.5	27
11	Correction of lung inflammation in a F508del CFTR murine cystic fibrosis model by the sphingosine-1-phosphate lyase inhibitor LX2931. American Journal of Physiology - Lung Cellular and Molecular Physiology, 2016, 311, L1000-L1014.	2.9	26
12	The effect of mirabegron on energy expenditure and brown adipose tissue in healthy lean South <scp>Asian and Europid</scp> men. Diabetes, Obesity and Metabolism, 2020, 22, 2032-2044.	4.4	25
13	Comprehensive single cell-resolution analysis of the role of chromatin regulators in early C. elegans embryogenesis. Developmental Biology, 2015, 398, 153-162.	2.0	24
14	Fully-automatic left ventricular segmentation from long-axis cardiac cine MR scans. Medical Image Analysis, 2017, 39, 44-55.	11.6	23
15	Treatment of rat congenital diaphragmatic hernia with sildenafil and NS-304, selexipag's active compound, at the pseudoglandular stage improves lung vasculature. American Journal of Physiology - Lung Cellular and Molecular Physiology, 2018, 315, L276-L285.	2.9	22
16	Time‣apse Imaging. , 2008, , 401-440.		21
17	Human Brown Adipose Tissue Estimated With Magnetic Resonance Imaging Undergoes Changes in Composition After Cold Exposure: An in vivo MRI Study in Healthy Volunteers. Frontiers in Endocrinology, 2019, 10, 898.	3.5	17
18	Extracellular Matrix Defects in Aneurysmal Fibulin-4 Mice Predispose to Lung Emphysema. PLoS ONE, 2014, 9, e106054.	2.5	17

ОLЕН DZYUBACHYK

#	Article	IF	CITATIONS
19	Super-resolution reconstruction of late gadolinium-enhanced MRI for improved myocardial scar assessment. Journal of Magnetic Resonance Imaging, 2015, 42, 160-167.	3.4	14
20	A VARIATIONAL MODEL FOR LEVEL-SET BASED CELL TRACKING IN TIME-LAPSE FLUORESCENCE MICROSCOPY IMAGES. , 2007, , .		12
21	Fast multistation water/fat imaging at 3T using DREAM-based RF shimming. Journal of Magnetic Resonance Imaging, 2015, 42, 217-223.	3.4	12
22	Interâ€station intensity standardization for wholeâ€body <scp>MR</scp> data. Magnetic Resonance in Medicine, 2017, 77, 422-433.	3.0	11
23	Automated Cardiovascular Segmentation in Patients with Congenital Heart Disease from 3D CMR Scans: Combining Multi-atlases and Level-Sets. Lecture Notes in Computer Science, 2017, , 147-155.	1.3	11
24	Automated algorithm for reconstruction of the complete spine from multistation 7T MR data. Magnetic Resonance in Medicine, 2013, 69, 1777-1786.	3.0	10
25	MRI Mouse Brain Data of Ischemic Lesion after Transient Middle Cerebral Artery Occlusion. Frontiers in Neuroinformatics, 2017, 11, 51.	2.5	9
26	Co-expression Patterns between ATN1 and ATXN2 Coincide with Brain Regions Affected in Huntington's Disease. Frontiers in Molecular Neuroscience, 2017, 10, 399.	2.9	9
27	Automated extraction and labelling of the arterial tree from whole-body MRA data. Medical Image Analysis, 2015, 24, 28-40.	11.6	8
28	Potential associations between immune signaling genes, deactivated microglia, and oligodendrocytes and cortical gray matter loss in patients with long-term remitted Cushing's disease. Psychoneuroendocrinology, 2021, 132, 105334.	2.7	6
29	Comparative exploration of whole-body MR through locally rigid transforms. International Journal of Computer Assisted Radiology and Surgery, 2013, 8, 635-647.	2.8	5
30	Increased Mortality and Vascular Phenotype in a Knock-In Mouse Model of Retinal Vasculopathy With Cerebral Leukoencephalopathy and Systemic Manifestations. Stroke, 2020, 51, 300-307.	2.0	5
31	Cingulate networks associated with gray matter loss in Parkinson's disease show high expression of cholinergic genes in the healthy brain. European Journal of Neuroscience, 2021, 53, 3727-3739.	2.6	5
32	Molecular characterization of the stress network in individuals at risk for schizophrenia. Neurobiology of Stress, 2021, 14, 100307.	4.0	5
33	Super-resolution reconstruction of whole-body MRI mouse data: An interactive approach. , 2012, , .		4
34	Joint Intensity Inhomogeneity Correction for Whole-Body MR Data. Lecture Notes in Computer Science, 2013, 16, 106-113.	1.3	3
35	Interactive Local Super-Resolution Reconstruction of Whole-Body MRI Mouse Data: A Pilot Study with Applications to Bone and Kidney Metastases. PLoS ONE, 2014, 9, e108730.	2.5	3
36	Computer-aided evaluation of inflammatory changes over time on MRI of the spine in patients with suspected axial spondyloarthritis: a feasibility study. BMC Medical Imaging, 2017, 17, 55.	2.7	2

ОLЕН DZYUBACHYK

#	Article	IF	CITATIONS
37	Transcriptomic Signatures Associated With Regional Cortical Thickness Changes in Parkinson's Disease. Frontiers in Neuroscience, 2021, 15, 733501.	2.8	2
38	Improved Myocardial Scar Characterization by Super-Resolution Reconstruction in Late Gadolinium Enhanced MRI. Lecture Notes in Computer Science, 2013, 16, 147-154.	1.3	2
39	Histogramâ€based standardization of intravascular optical coherence tomography images acquired from different imaging systems. Medical Physics, 2018, 45, 4158-4170.	3.0	1
40	The Effect Of Mirabegron On Energy Expenditure, Brown Adipose Tissue And The Lipidomic Profile In Healthy Lean South Asian And White Caucasian Men. Atherosclerosis, 2019, 287, e279.	0.8	1
41	Stochastic neighbor embedding as a tool for visualizing the encoding capability of magnetic resonance fingerprinting dictionaries. Magnetic Resonance Materials in Physics, Biology, and Medicine, 2021, , 1.	2.0	1
42	Biosensor for deconvolution of individual cell fate in response to ion beam irradiation. Cell Reports Methods, 2022, 2, 100169.	2.9	1
43	Development of Next Generation Biomedical Sensor for Single Cell Four Dimensional Tracing of Cellular Response to Ion Beam Irradiation. SSRN Electronic Journal, 0, , .	0.4	0
44	On the ability to exploit signal fluctuations in pseudocontinuous arterial spin labeling for inferring the major flow territories from a traditional perfusion scan. NeuroImage, 2021, 230, 117813.	4.2	0